Multiple self-assembled nanostructures from an oligo(*p*-phenyleneethynylene) containing rod–coil–rod triblock copolymer†

Kun Li and Qing Wang*

Received (in Columbia, MO, USA) 8th May 2005, Accepted 2nd August 2005
First published as an Advance Article on the web 25th August 2005
DOI: 10.1039/b506463e

Induced by systematic variation of the initial polymer concentration in toluene, various morphologies of aggregates including vesicles, spheres, onion-like structures, and worm-like fibers from a rod–coil–rod triblock copolymer, oligo(*p*-phenyleneethynylene)–polystyrene–oligo(*p*-phenyleneethynylene), were observed by transmission electron microscopy.

Self-assembly of block copolymers has been demonstrated as a powerful route towards supramolecular objects with novel architectures, functions and properties.[1] Of particular recent interest are rod–coil block copolymers composed of π-conjugated polymer chains as the rod-like component. The incorporation of conjugated polymers into block copolymer architectures opens the way for the tuning of both molecular organization and the electronic and optical properties of these materials by controlling their aggregation behavior.[2–4] However, compared to conventional coil–coil block copolymers, there has been limited success in gaining control over the morphologies of conjugated rod–coil block copolymers through systematic variation of the chemical composition and/or utilization of external stimuli such as temperature and solvent. Recently, diverse ordered aggregates from amphiphilic rod–coil diblock copolymers, poly(phenylquinoline)–polystyrene have been generated through the manipulation of polymer structures and solvent quality.[5] The breath figure method led to highly ordered, microporous honeycomb structures from the rod–coil copolymers.[6] In this Communication, we present the remarkable change in aggregate morphologies of a rod–coil–rod triblock copolymer, oligo(*p*-phenyleneethynylene)–polystyrene–oligo(*p*-phenyleneethynylene) (OPE–PS–OPE). Depending on the initial polymer concentration in toluene, OPE–PS–OPE has been shown to self-organize into a series of morphologies including vesicles, onion-like structures, spheres and rod-like fibers.

The synthetic approach to the triblock structure OPE–PS–OPE is depicted in Scheme 1. Starting from 1-bromo-4-iodobenzene, a phenyleneethynylene trimer, **4**, with amino and iodo end groups was prepared in four steps. The presence of the terminal amine functionality allows the coupling of **4** to a monodispersed α,ω-dicarboxyl-terminated polystyrene (**5**) to yield compound **6**. Condensation of **6** with 2 equiv. of 1-ethynyl-4-(phenylethynyl)-benzene (**7**) using $Pd(PPh_3)_2Cl_2$ and CuI as the catalysts afforded OPE–PS–OPE. The number-average molecular weights of compound **6** and OPE–PS–OPE, analyzed against polystyrene standards by Waters gel permeation chromatography (GPC) using THF as the eluent, were determined to be 5530 and 6100 Da with polydispersities of 1.14 and 1.15, respectively. The structures of the polymers were confirmed by spectroscopic studies and elemental analysis. In the ^{1}H NMR spectrum of compound **6**, the signals observed at 7.69 and 7.49 ppm are assignable to benzylic protons from oligo(*p*-phenyleneethynylene) (OPE) segments. On the other hand, a signal at 3.92 ppm corresponding to amino groups from compound **4** was not detected. The ethine carbons from OPE are found at 90–94 ppm in the ^{13}C NMR spectrum of compound **6**. In the ^{1}H NMR spectrum of OPE–PS–OPE, the increased intensity of a singlet at 7.49 ppm and the absence of a doublet at 7.69 ppm corresponding to aromatic protons adjacent to the iodo group indicate the presence of pentameric OPE in the triblock copolymer. The Raman peaks of OPE–PS–OPE are located around 1118, 1591 and 2210 cm^{-1}, and are ascribed to triple bond stretching of the OPE pentamer. The UV-vis spectra show that the π–π* transition of the conjugated backbones, observed in compound **4** at 345 nm, was blue-shifted to 335 nm for compound **6** because of the electron withdrawing effect of amide

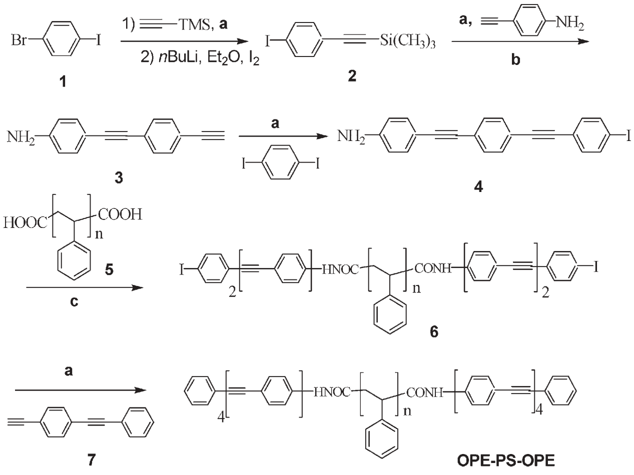

Reagents: **a**. $PdCl_2(PPh_3)_2$ (3 mol%), CuI (1 mol%), Et_3N/THF (1:1)
b. K_2CO_3, CH_3OH, CH_2Cl_2
c. i) $SOCl_2$, reflux 5 hours; ii) **4**, THF/ pyridine (2:1)

Scheme 1 Synthesis of the triblock copolymer OPE–PS–OPE.

Department of Materials Science and Engineering, The Pennsylvania State University, University Park, Pennsylvania 16802, USA.
E-mail: wang@matse.psu.edu; Fax: +1 814-865-2917;
Tel: +1 814-863-0042

† Electronic supplementary information (ESI) available: Experimental procedures and characterization data for the synthesized compounds. See http://dx.doi.org/10.1039/b506463e

bonds. The absorption maximum of OPE–PS–OPE appears at 363 nm due to the increase in conjugation length.

A remarkable self-assembly process to form various aggregates that have not been observed from phenyleneethynylene-containing copolymers[7] was achieved simply by the direct dissolution of the block copolymer OPE–PS–OPE in toluene. Given the fact that toluene is a good solvent for the polystyrene (PS) block but a precipitant for unsubstituted OPE segments,[3c] OPE–PS–OPE is prone to form micelle-like aggregates consisting of a packed OPE core and a PS corona shell. As shown in Fig. 1, even at a very low concentration of 10^{-3} mg mL^{-1}, the emission spectrum of OPE–PS–OPE displays a pronounced peak at 391 nm coming from the solvated polymer chains and a red-shifted one at 415 nm. The band at 415 nm is believed to originate from the formation of excimers, which are induced by the intramolecular and/or intermolecular folding of OPE blocks.[8] To observe the aggregate morphologies under transmission electron microscopy (TEM), dilute solutions of OPE–PS–OPE in toluene were deposited onto carbon-coated copper grids. After the evaporation of toluene at atmospheric pressure and room temperature, the cast films were investigated by a Phillips EM410 electron microscope operated at an acceleration voltage of 80 kV. Typical morphologies observed by TEM for the solutions at various initial polymer concentrations are shown in Fig. 2. These images were obtained without staining the sample. When the initial concentration of OPE–PS–OPE is 0.20 mg mL^{-1}, vesicular structures were detected, as evidenced from a higher transmission in the center of the aggregates than their periphery in the TEM picture (Fig. 2A). The wall thickness of the vesicles is very uniform, at about 15 nm, and independent of the overall size of the vesicles. Since the lengths of the OPE block and PS coil are about 3.5 and 5.5 nm, respectively, the wall thickness of the vesicles roughly corresponds to twice the length of a folding OPE–PS–OPE molecule, indicating a bilayer lamellar packing of the OPE blocks. Further evidence for the lamellar was obtained from the absorption and emission spectroscopic experiments. With the polymer concentration increasing over the range 0.2 to 0.5 mg mL^{-1}, the relative intensity of the peak at 391 nm dramatically decreases, while the intensity of the band at 415 nm increases, confirming that the peak at 415 nm originates from excimers produced by the intramolecular and/or intermolecular π electronic coupling of the OPE aggregates. Accordingly, the photoluminescence quantum yield drops from 0.78 to 0.60 as shown in the inset of Fig. 1. For the thin film cast from 2.0 mg mL^{-1} solution, the absorption maximum resulting from the OPE block was blue-shifted from 363 nm in toluene to 343 nm. This 20 nm hypsochromic shift is substantial, and seldom found from phenyleneethynylene based assembly structures. We note that such a hypsochromic shift has been observed from short unsubstituted oligothiophenes and α,ω-substituted oligothiophenes in Langmuir–Blodgett and vacuum-deposited thin films, suggesting the orientation of the conjugated blocks with their long axes parallel to each other (*e.g.* H-aggregates).[9,10] Herein, the resulting hypsochromic shift from OPE–PS–OPE copolymer thin films can be interpreted by the molecular exciton model,[11] and also indicates lamellar structures with an orientation parallel to the OPE segments.

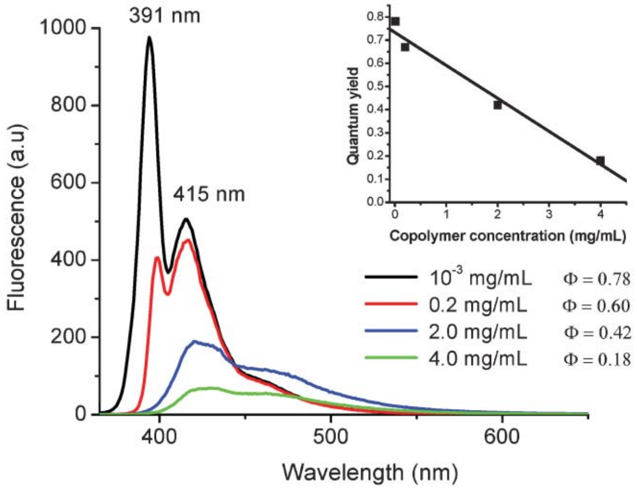

Fig. 1 Fluorescence spectra of the triblock copolymer in toluene. The inset shows the photoluminescence quantum yield (*Φ*) as a function of the copolymer concentration.

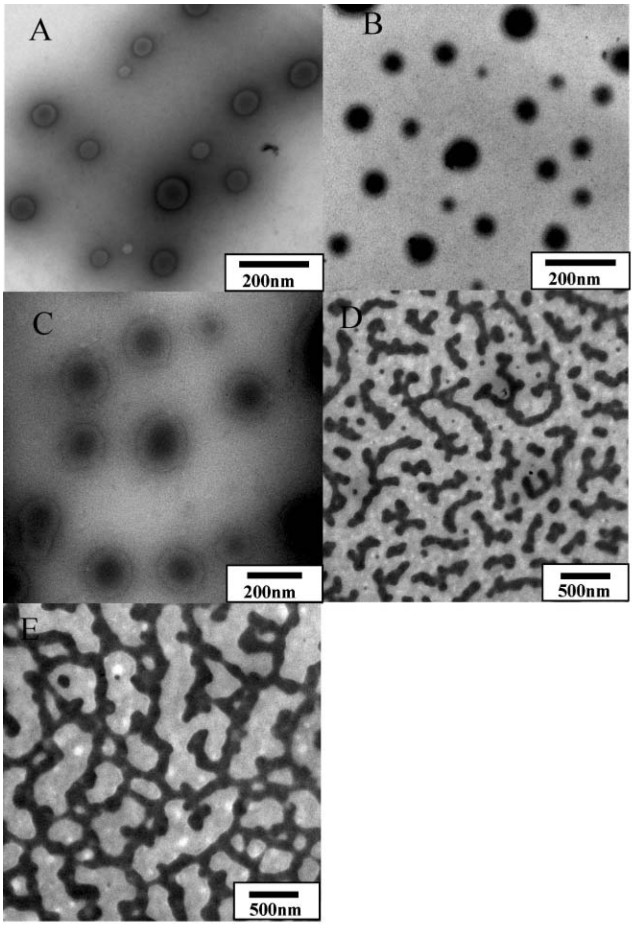

Fig. 2 TEM micrographs of OPE–PS–OPE from toluene solution: A. 0.2 mg mL^{-1}; B. 2.0 mg mL^{-1}; C. 2.5 mg mL^{-1}; D. 4.0 mg mL^{-1}; E. 5.0 mg mL^{-1}.

As the polymer concentration increases to 2.0 mg mL^{-1}, the photoluminescence spectrum reveals that the aggregation band at 415 nm is fully developed and the peak at 391 nm disappears completely. Interestingly, the increased polymer concentration leads to a morphological transition from vesicles to spherical micelles. As shown in Fig. 2B, the uniformity of the light intensity over the entire feature supports the spherical nature of micelles. These transitions in aggregation structures can be intuitively understood in terms of the packing requirements of the OPE block in the selective solvent toluene. With the progressive increase of the polymer concentrations, the spontaneous formation of large aggregates with a dense concentric lamella structure is favored because it considerably decreases the interface area between toluene and the aggregating OPE blocks.[12] The proposed lamellar structure is further proved by the detection of onion-like micelles coexisting with the spheres from a higher polymer concentration at 2.5 mg mL^{-1} (Fig. 2C). The comparable shrinking rates of OPE and PS layers and muti-lamellar structures result in the onion architecture, which is considered to be controlled largely by the same thermodynamics that lead to the formation of the lamellar phase in bulk.[13] The thickness of the outermost shell as determined from TEM is very uniform, at around 15 nm, still corresponding well with the bilayer structure of the folding OPE–PS–OPE.

When the initial polymer concentration is increased to 4.0 mg mL^{-1}, another structural transition occurs, as shown by the formation of worm-like micelles in Fig. 2D. The resulting morphological change is presumably due to coalescence of spheres into cylinders. The micrograph suggests a relatively narrow size distribution of the cylindrical micelle diameters. Consequently, the aggregate emission peak is further red-shifted from 415 to 421 nm, accompanied by quenched emission intensity and a reduced quantum yield because of the presence of densely packed aggregates. Upon a further increase of the initial polymer concentration to 5 mg mL^{-1}, interconnected rod-like fibers appear as shown in Fig. 2E. The observed aggregate characteristics are proposed to result from the adhesion, collision and fusion of worm-like micelles at high polymer concentrations.

The formation of aggregates is likely the outcome of the cooperative effect of microphase separation in the selective solvent and self-assembly driven by π-stacking and hydrogen bonding interactions. Without the steric repulsion from α-position substituents, the rigid OPE block is inclined to form the folding structure *via* aromatic π–π interactions. With the segregation of the OPE core, the distance between amide groups in OPE–PS–OPE decreases and facilitates the formation of hydrogen bonds, which can further enforce the lamellar packing of OPEs and strengthen the molecular self-assembly process. The effect of concentration on morphology can be explained using basic concepts of crystal growth. The nucleation sites, *i.e.* the number and dimension of aggregates, increases with concentration, as seen in the blue-shifted absorption and quenched fluorescence spectra. The growth rate is controlled by the diffusion process, and hence, at higher concentration, the probability that the molecules encounter each other increases. Consequently, larger aggregates are formed in concentrated solution than in dilute solution. Therefore, it is also not surprising to note that the morphologies of OPE–PS–OPE are also strongly dependent upon the solvent evaporation conditions. In the case of fast evaporation and the thin films prepared by spin-coating, only "random" morphologies without any indications of long-range order have been observed. These phenomena might result from the fact that the high rate of solidification under these accelerated evaporation conditions changed the growth rates and kinetically suppressed the intrinsic self-assembly of OPEs driven by π–π aromatic interactions. Reversibility between the different morphologies has also been observed. In other words, the same aggregate can be obtained from either dilute solution or dilution of relatively concentrated solution with a different morphology.

In summary, we present here a simple solution-based route for the control of morphology in a rod–coil–rod conjugated polymer. As elucidated in TEM studies, the transitions in aggregation morphologies are found to be correlated with the initial concentration of the polymer. Our understanding of this subject is still qualitative, but the evidence obtained suggests that one can exercise control over conjugated polymer morphologies through the interplay between nonspecific interactions, *i.e.* demixing of rigid and flexible polymer parts, and self-organization driven by specific attractive forces such as aromatic π-stacking and hydrogen bonding. The study of the formation of multiple phase behavior within a single structure is interesting because it may provide unprecedented insight into the factors controlling the self-assembling architecture of conjugated block copolymers. It also allows for the study of electronic and optical property correlations as a function of structure. These studies, as well as complete investigations of these unique assemblies, are current in progress.

This work was supported by The Pennsylvanian State University.

Notes and references

1 (*a*) S. I. Stupp, V. Lebonheur, K. Walker, S. L. Li, K. E. Huggins, M. Keser and A. Amstutz, *Science*, 1997, **276**, 384; (*b*) J. T. Chen, E. T. Thomas, C. K. Ober and G. P. Mao, *Science*, 1996, **273**, 343; (*c*) S. Jain and F. S. Bates, *Science*, 2003, **300**, 460; (*d*) Z. Li, E. Kesselman, Y. Talmon, A. Hillmyer and T. P. Lodge, *Science*, 2004, **306**, 98; (*e*) H. A. Klok and S. Lecommandoux, *Adv. Mater.*, 2001, **13**, 1217.

2 (*a*) M. Lee, B. K. Cho and W. C. Zin, *Chem. Rev.*, 2001, **101**, 3869; (*b*) G. Widawshi, M. Rawiso and B. Francois, *Nature*, 1994, **369**, 387; (*c*) U. Stalmach, B. de Boer, C. Videlot, P. F van Hutten and G. Hadziioannou, *J. Am. Chem. Soc.*, 2000, **122**, 5464; (*d*) H. Wang, H. H. Wang, V. S. Urban, K. C. Littrel, P. Thiyagarajan and L. Yu, *J. Am. Chem. Soc.*, 2000, **122**, 6855; (*e*) J. Liu, E. Sheina, T. Kowalewski and R. D. McCullough, *Angew. Chem., Int. Ed.*, 2002, **41**, 329; (*f*) J. F. Hulvat, M. Sofos, K. Tajima and S. I. Stupp, *J. Am. Chem. Soc.*, 2005, **127**, 366.

3 (*a*) M. A. Hempenius, B. M. W. Langeveld-Voss, J. A. E. H. van Haar, R. A. J. Janssen, S. S. Sheiko, J. P. Spatz, M. Möller and E. W. Meijer, *J. Am. Chem. Soc.*, 1998, **120**, 2798; (*b*) H. Kukula, U. Ziener, M. Schol and A. Godt, *Macromolecules*, 1998, **31**, 5160; (*c*) K. Li and Q. Wang, *Macromolecules*, 2004, **37**, 1172.

4 (*a*) K. Nawa, I. Imae, N. Noma and Y. Shirota, *Macromolecules*, 1995, **28**, 723; (*b*) T. Hayakawa and S. Horiuchi, *Angew. Chem., Int. Ed.*, 2003, **42**, 2285.

5 (*a*) S. Jenekhe and X. L. Chen, *Science*, 1998, **279**, 1903; (*b*) S. Jenekhe and X. L. Chen, *Science*, 1999, **283**, 372.

6 B. Boer, U. Stalmach, H. Nijland and G. Hadziioannou, *Adv, Mater.*, 2000, **12**, 1581.

7 (*a*) P. Samori, V. Francke, K. Mullen and J. P. Rabe, *Chem. Eur. J.*, 1999, **5**, 2312; (*b*) C. A. Breen, T. Deng, T. Breiner, L. Edwin and T. M. Swager, *J. Am. Chem. Soc.*, 2003, **125**, 9942; (*c*) Y. Q. Wang, J. N. Wilson, M. D. Smith and U. H. F. Bunz, *Macromolecules*, 2004, **37**, 9701.

8 U. H. F. Bunz, *Chem. Rev.*, 2000, **100**, 1605.

9 U. Schoeler, K. H. Tew and H. Kuhn, *J. Chem. Phys.*, 1974, **61**, 5009.

10 (*a*) A. Yassar, G. Horowitz, P. Valat, V. Wintgens, M. Hymene, F. Deloffre, P. Sirvastava, P. Lang and F. Garnier, *J. Phys. Chem.*, 1995, **99**, 9915; (*b*) S. Hotta and K. Waragai, *J. Phys. Chem.*, 1993, **97**, 7427.

11 (*a*) A. Yassar, P. Valat and V. Wintgens, *J. Phys. Chem.*, 1995, **99**, 9155; (*b*) A. B. Koren, M. D. Curtis, A. H. Francis and J. W. Kampf, *J. Am. Chem. Soc.*, 2003, **125**, 5040.

12 H. Shen and A. Eisenberg, *Angew. Chem., Int. Ed.*, 2000, **39**, 3310.

13 K. Prochazka, T. J. Martin, S. E. Webber and P. Munk, *Macromolecules*, 1996, **29**, 6526.